Amorphous Silicon with Extremely Low Absorption: Beating Thermal Noise in Gravitational Astronomy

R. Birney,[1,2,*] J. Steinlechner,[3,4,†] Z. Tornasi,[3] S. MacFoy,[1,2] D. Vine,[2] A. S. Bell,[3] D. Gibson,[2] J. Hough,[3] S. Rowan,[3] P. Sortais,[5] S. Sproules,[6] S. Tait,[3] I. W. Martin,[3] and S. Reid[1,2]

[1]*SUPA, Department of Biomedical Engineering, University of Strathclyde, Glasgow G1 1QE, United Kingdom*
[2]*SUPA, Institute for Thin Films, Sensors and Imaging, University of the West of Scotland, Paisley PA1 2BE, United Kingdom*
[3]*SUPA, Institute for Gravitational Research, University of Glasgow, Glasgow G12 8QQ, United Kingdom*
[4]*Institut für Laserphysik und Zentrum für Optische Quantentechnologien, Universität Hamburg, Luruper Chaussee 149, 22761 Hamburg, Germany*
[5]*Polygon Physics, 30 Chemin de Rochasson, 38240 Meylan, France*
[6]*WestCHEM, School of Chemistry, University of Glasgow, Glasgow G12 8QQ, United Kingdom*

(Received 9 July 2018; revised manuscript received 23 August 2018; published 6 November 2018)

Amorphous silicon has ideal properties for many applications in fundamental research and industry. However, the optical absorption is often unacceptably high, particularly for gravitational-wave detection. We report a novel ion-beam deposition method for fabricating amorphous silicon with unprecedentedly low unpaired electron-spin density and optical absorption, the spin limit on absorption being surpassed for the first time. At low unpaired electron density, the absorption is no longer correlated with electron spins, but with the electronic mobility gap. Compared to standard ion-beam deposition, the absorption at 1550 nm is lower by a factor of ≈100. This breakthrough shows that amorphous silicon could be exploited as an extreme performance optical coating in near-infrared applications, and it represents an important proof of concept for future gravitational-wave detectors.

DOI: 10.1103/PhysRevLett.121.191101

Introduction.—Highly reflective optical coatings have a wide range of applications in research and technology. Ultrastable optical cavities are essential components in atomic clocks, which are revolutionizing time and frequency standards and measurement [1–3]. Ultrastable cavities also form the heart of a gravitational-wave detector. The measurement of gravitational waves is an exciting tool for astrophysics, making dark objects such as black holes visible [4–7]. In all of these applications, performance is currently limited by Brownian thermal noise, which is proportional to the mechanical loss and thickness of the mirror coatings [8–11].

Amorphous silicon (*a*-Si) is a highly interesting coating material due to low mechanical loss at room temperature, which decreases toward low temperatures [12,13], and a very high refractive index of approximately $n = 3.5$ in the near-infrared (NIR). Highly reflective dielectric mirror coatings comprise alternating layers of materials with low and high n. Typically, the layers are a quarter of the design wavelength in optical thickness [quarter-wave optical thickness (QWOT)], optical thickness being equal to nd, where d is physical thickness of the layer, two of the most commonly used wavelengths being 1064 and 1550 nm. Compared to materials of lower n, the high index of *a*-Si allows fewer layers to be deposited in order to achieve the same reflectivity, due to a higher refractive index contrast Δn between the two materials. Additionally, the quarterwave thickness is directly reduced.

To avoid heating and thermal deformation of the mirrors in gravitational-wave detectors, or to realize ultrahigh finesse cavities, low optical absorption at the ppm (10^{-6}) level is required. However, the optical absorption of *a*-Si may be significantly higher [14]. Recent research has resulted in an absorption reduction of more than a factor of 50 when using *a*-Si at a wavelength of 2 μm, and at low temperatures [15,16]. However, shorter wavelengths are preferable, because an increase in wavelength increases the coating thickness by the ratio of the wavelengths, and therefore coating thermal noise by the square root of the ratios. In addition, the telecommunication wavelength of 1550 nm is attractive, due to the ready availability of high power lasers and optical components.

Incorporating hydrogen into *a*-Si has been reported to significantly reduce optical absorption [17]. However, hydrogenation may be undesirable due to reduction of the refractive index and may result in the formation of infrared absorbing hydroxyl (OH) groups when combined with frequently used low-n oxide materials (e.g., SiO_2).

In this Letter, we describe a novel ion-beam deposition (IBD) process for fabricating hydrogen-free low-absorbing *a*-Si coatings. We show that it is possible to reduce the number of unpaired electrons to a level at which they no longer significantly contribute to absorption. In this regime, absorption remains correlated with the electronic mobility gap. We investigate the optimum heat-treatment

temperature and the effect of elevated temperature deposition on the material. The optical absorption reaches a minimum upon heat treatment at 400 °C, while mechanical dissipation at room temperature is minimized by deposition at 200 °C, followed by postdeposition heat treatment at 400 °C.

The lowest absorption achieved corresponds to an extinction coefficient of $k = (1.2 \pm 0.2) \times 10^{-5}$ at 1550 nm and of $k = (1.7 \pm 0.1) \times 10^{-4}$ at 1064 nm. This is approximately 25× lower at 1064 nm, and more than 100× lower at 1550 nm [15], than previously reported for IBD-deposited thin films.

Coating deposition.—IBD is commonly used to produce the highest-quality optical coatings with low optical absorption and scatter. The *a*-Si coatings investigated here were produced by a custom-built IBD system (see Fig. 1), incorporating a novel electron cyclotron resonance (ECR) ion source [18].

The ion beam is formed by injection of argon gas into a resonant microwave cavity where it is ionized via ECR [19]. The cavity was tuned to 2.45 GHz, and the microwave power was held constant at 11.6 W. In conventional IBD, the cavity walls are held at high voltage and the ions are extracted through a grid. The higher frequency of ECR sources [20,21] enables generation of a more highly confined plasma, which can be extracted through a single aperture. This reduces the possibility of contamination from the grid material and permits extraction potentials an order of magnitude larger (11.7 kV in this Letter).

The deposition rate used here of ∼0.05 Å/s is ≈20 times lower than for conventional IBD. Deposition rate is known to affect atomic structure during thin film growth [22,23] and therefore may play an important role in reducing the density of undercoordinated Si atoms.

a-Si coatings were deposited using an *N*-type (phosphorus doped) crystalline silicon (semiconductor grade) target with resistivity = 1–10 Ω cm. Base pressure in the chamber prior to deposition was a maximum of 1×10^{-6} mbar (averaging 5×10^{-7} mbar) and 8×10^{-5} mbar during deposition. Coatings were deposited in a newly built vacuum chamber; no other coating materials had previously been produced in this system, and the deposition environment was therefore largely free of potential contaminants. Elemental analysis was conducted via energy-dispersive X-ray spectroscopy, using room-temperature deposited *a*-Si films on GaAs substrates. The oxygen content was quantified to be ≤ 5%, consistent with that expected from the slow deposition rate and base pressure in the coating chamber. SiH and SiH_2 content was estimated to be < 1% with Raman spectroscopy [24].

Optical absorption measurements.—Substrates made of Corning 7979 [25] and JGS-1 [26] fused silica, which show negligible optical absorption at 1064 and 1550 nm, were coated for absorption measurements. During the coating process, the substrates were mounted on a stage with heating capability. Coatings were deposited at room temperature (with an initial substrate temperature of 20 °C, increasing to 35 °C after 1-hour deposition) and at elevated substrate temperatures of 200 and 400 °C.

Optical absorption of the *a*-Si films was measured using photothermal common-path interferometry (PCI) [27]. Accounting for interference effects, the extinction coefficient *k* was calculated [28].

Figure 2 shows *k* at 1550 nm of a room-temperature deposited *a*-Si sample as a function of postdeposition heat-treatment temperature. The sample was heat treated for 1 hour in air for each heat-treatment step. *k* shows a minimum of $(1.22 \pm 0.21) \times 10^{-5}$ after heat treatment at 400 °C. This corresponds to an absorption of a highly reflective $a\text{-Si}/SiO_2$ stack of (7.6 ± 1.4) ppm, assuming negligible absorption in the SiO_2 layers [15]. A commercial *a*-Si coating produced via IBD by *Advanced Thin Films* is shown for comparison (data from Ref. [15]).

Figure 3 shows *k* at 1550 nm as a function of deposition temperature. Each sample was measured after deposition and then heat treated at 400 °C for 3 hours (except for the points taken from Fig. 2). For room-temperature deposition, *k* shows a wide spread for nominally identical deposition parameters. However, on average, a general decreasing trend of *k* with deposition temperature is

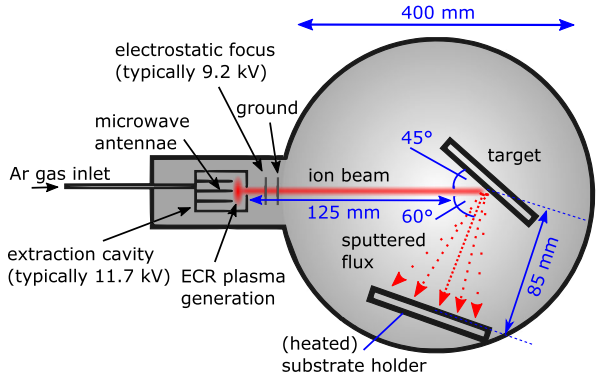

FIG. 1. Schematic of the deposition setup for producing ultra-low absorbing *a*-Si.

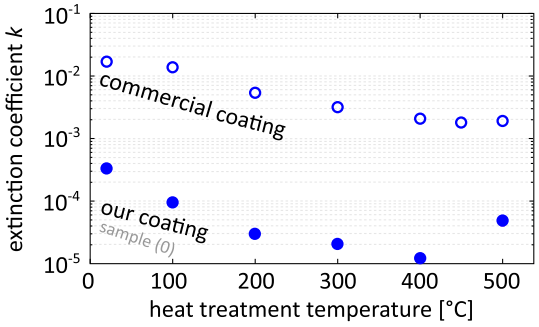

FIG. 2. Extinction coefficient *k* at 1550 nm as a function of heat treatment temperature for our coating and, for comparison, of a commercial coating (data from Ref. [15]).

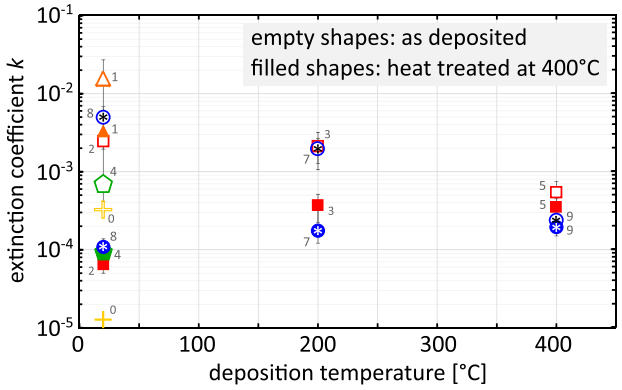

FIG. 3. Extinction coefficient k at 1550 nm as a function of deposition temperature. At each temperature, different coatings are indicated by different shapes. (Crosses represent our coating from Fig. 2; stars indicate coatings deposited on Corning 7979 substrates; all other coatings were deposited on JGS-1 substrates.)

observable for the as-deposited samples, and all individual samples show a decrease in k following heat treatment. We note that postdeposition heat treatment can result in lower k values than elevated-temperature deposition at the same temperature alone. The improvement with postdeposition heat treatment at deposition temperature is small. We assume that the spread in absorption for films deposited under nominally identical conditions arises from an unknown variation in deposition parameters, most likely chamber cleanliness. Because the coatings with the lowest absorption were among the first produced in the IBD system following commissioning and testing, it seems likely that absorption variations may be related to accumulating contamination of the coating chamber.

Optical absorption mechanisms.—Unpaired electrons are known to contribute to the absorption in a-Si [29]. The density of unpaired electrons ("spin density") of several samples was measured via electron paramagnetic resonance (EPR) [30]. Figure 4 shows k versus number of

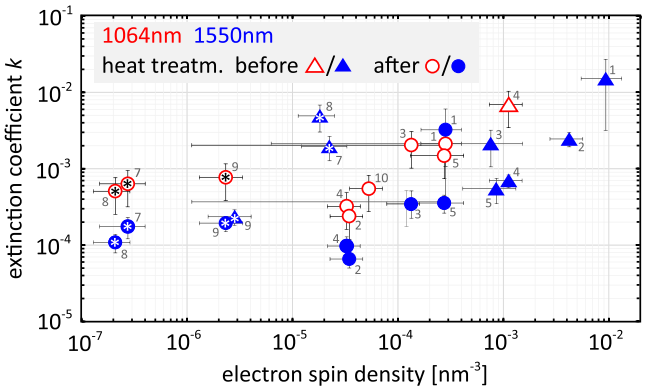

FIG. 4. Extinction coefficient k at 1064 nm (red) and 1550 nm (blue) of a-Si coatings as a function of electron-spin density. Stars (*) indicate coatings on Corning 7979 substrates; all other coatings were on JGS-1.

electron spins per nm^3 for a variety of samples, some of which were deposited at room temperature, some at elevated temperature, and some were heat treated at 400 °C after deposition. The absorption was measured for the same samples at both 1064 and 1550 nm (several samples were not measured at 1064 nm before heat treatment, as they had already been heat treated for the 1550 nm measurements), and we note the evidence of substrate effects in these measurements which warrants further investigation.

Both heat treatment and high temperature deposition can be observed to reduce the spin density, in addition to the previously noted reduction in absorption. Samples 4 and 9, which were deposited and heat treated at 400 °C, show little or no significant change in spin density following heat treatment—consistent with the minimal reduction in absorption in these samples following heat treatment at deposition temperature. When considering all samples, a decrease in k with decreasing spin density is observed for spin densities above $\approx 4 \times 10^{-5}/\mathrm{nm}^3$, with broadly linear dependence, in good agreement with other studies [17]. However, we observe that when the spin density is reduced below $\approx 4 \times 10^{-5}/\mathrm{nm}^3$, no further decrease in absorption is observed. This indicates that another absorption mechanism dominates in this regime. It is interesting to note that the spin density typically observed in nonhydrogenated a-Si [31,32] is in the order of 5×10^{-3} nm^{-3}, significantly higher than observed in the majority of our ECR-IBD films.

The relationship between absorption and electronic structure in the low-spin density regime in Fig. 4 was investigated through analysis of the a-Si coatings' transmittance spectra between 200 and 2000 nm.

Spectra were analyzed using the software package SCOUT [33], with the dielectric function of a-Si modeled as the sum of a constant dielectric background [34], an O'Leary, Johnson and Lim (OJL) term [35] to model interband transitions, and an extended Drude term [36] representing electron transport properties. The dielectric function of the substrate was calculated separately, allowing the total transmittance of a-Si on fused silica to be modeled and fitted to the measured spectrum.

The fitting parameter of interest to this study is the OJL mobility gap, E_g, which is related to the position of the transmittance-spectrum absorption edge. The localized-state decay constants were taken to be identical for the valence and conduction bands ($\gamma_{\mathrm{val}} = \gamma_{\mathrm{cond}}$). The lowest optical absorption is observed in the "plateau" region not dominated by electron spins in Fig. 4. A correlation is suggested between extinction coefficient and mobility gap (Fig. 5), in agreement with the hypothesis that the mechanism for absorption is interband transitions rather than absorption by defects, impurities, or dangling bonds. No correlation was observed with γ, indicative of the degree of disorder (there are various types and degrees of disorder that are known to affect the mobility gap edges in a-Si

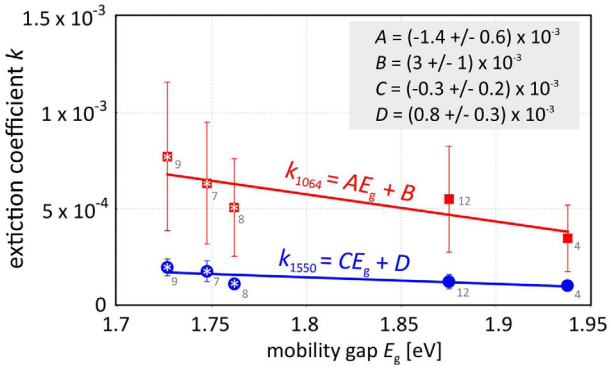

FIG. 5. Extinction coefficient k as a function of the calculated mobility gap energy from the OJL model for absorption results in the plateau region of Fig. 4, with linear fit. Stars indicate coatings on Corning 7979 substrates; all other coatings were on JGS-1.

[37]). The value of γ obtained from all fits was very similar, with an average value of 0.12 ± 0.02.

It is known that E_g for an amorphous semiconductor decreases as the average atomic spacing increases [38]. Thus, a further decrease in this remarkably low absorption may be possible through decreasing the average atomic spacing via optimization of deposition parameters, specifically, increased extraction potential, i.e., higher ion energy (see *Coating Deposition* Section for parameters used), or the incorporation of addition processes known to improve densification, e.g., ion assist.

Thermal noise performance.—To estimate the thermal noise performance of these coatings, fused silica cantilevers were coated at the same temperatures as the disc samples, to facilitate studies of the mechanical loss. Coating mechanical loss may be calculated from the difference between the free amplitude decay of the cantilevers' resonant modes before and after coating [39].

Figure 6 shows the coating mechanical loss as a function of deposition temperature. The purple squares show the average loss of several bending modes of the as-deposited coating, and the green circles show the average loss of the coating after heat treatment at 400 °C. The lowest coating

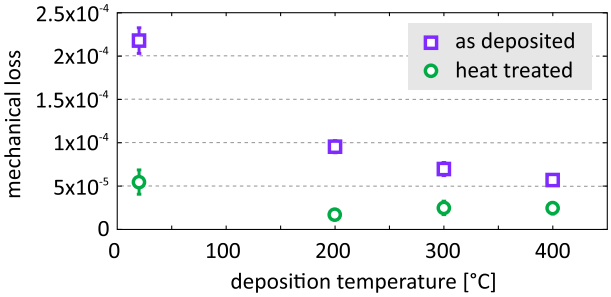

FIG. 6. Coating mechanical loss as a function of deposition temperature: Each point represents the average loss of several resonant modes (purple squares: coating as deposited, green circles: heat treatment for 1 hour at 400 °C).

TABLE I. Thermal noise possible when using ECR-IBD a-Si in a multimaterial coating compared to Advanced LIGO. The numbers are for ETMs with a beam diameter of 6.2 cm and in parenthesis for the ITMs with a beam diameter of 5.5 cm as used in Advanced LIGO. Mechanical loss values used for $Ti:Ta_2O_5$ and SiO_2 are taken from Ref. [40].

Thermal noise [a] [%]	Absorption (ppm)	No. of bilayers $Ti:Ta_2O_5/SiO_2$	ETM (ITM) a-Si/SiO_2
Baseline Advanced LIGO (a)			
100	≈0.3 (0.2) [41]	18.5 (9.5)	0 (0)
a-Si/SiO_2 1550 nm (b)			
29.9	7.6	…	7.5 (4.5)
Multimaterial 1550 nm (c)			
49.5	2.1 (2.0)	2 (2)	6.5 (2.5)

[a]For whole detector

loss of $\phi = (1.7 \pm 0.1) \times 10^{-5}$ was found for deposition at 200 °C followed by postdeposition heat treatment at 400 °C. No frequency dependence was observed, with the losses approximately a factor of 5 lower than that previously reported for identically treated a-Si coatings deposited by conventional IBD [12].

Table I compares thermal noise for different coatings used in the Advanced Laser Interferometer Gravitational-Wave Observatory (LIGO) detectors. The total thermal noise has contributions from two cavity input mirrors (ITMs) and two cavity end mirrors (ETMs). Thermal noise of the current Advanced LIGO coatings, consisting of Ta_2O_5 doped with TiO_2 ($Ti:Ta_2O_5$) and SiO_2 at a wavelength of 1064 nm [coating (a)], is defined as 100%. Using SiO_2 together with the lowest absorption and mechanical loss found for our a-Si at 1550 nm [coating (b)] reduces thermal noise to 29.9% that of coating (a) for similar mirror transmissions.

Although being remarkably low for a-Si, the absorption of 7.6 ppm is still above the tolerable level for use in gravitational-wave detectors. In the silica Advanced LIGO mirrors, tolerable levels of thermal distortion may suggest a maximum coating absorption of 2.5 ppm [42,43]. A method of further reducing the absorption of coating (b) is a "multimaterial" design, in which low-absorbing $Ti:Ta_2O_5/SiO_2$ layers on top of the coating reduce the laser power before it arrives at the a-Si layers [44,45]. Depending on the number of $Ti:Ta_2O_5/SiO_2$ layers, absorption in the a-Si may be tuned. However, this tuning requires a trade-off between absorption reduction and thermal noise increase due to the higher mechanical loss of $Ti:Ta_2O_5/SiO_2$. Using two bilayers of $Ti:Ta_2O_5/SiO_2$ reduces the absorption to < 2.5 ppm, with a slight increase in thermal noise to 49.5% of coating (a). This meets the Advanced LIGO Plus requirement of a factor of two reduction in thermal noise [46].

Conclusion.—We have developed a process for depositing hydrogen-free *a*-Si films with unprecedentedly low electron-spin density. The absorption is correlated with the electron-spin density for densities above $\approx 1 \times 10^{-5}/\ \mathrm{nm}^3$, below which it is correlated with the electronic mobility gap. Films with optical absorption a factor of ≈100 lower at 1550 nm (≈25× lower at 1064 nm), compared to conventional IBD *a*-Si, have been produced. The mechanical loss after optimal heat treatment is ≈5× lower than for *a*-Si deposited by conventional IBD.

The very low optical absorption and mechanical loss enable the use of *a*-Si for significant thermal noise reduction in precision measurements. A multimaterial design can reduce coating thermal noise to 49.5% of the Advanced LIGO level, for a change in wavelength to 1550 nm, while keeping the absorption < 2.5 ppm. This provides, for the first time, a route to significant sensitivity improvement at room temperature, exceeding the requirements for the planned Advanced LIGO Plus detector [46], designed to increase detection rates by a factor of ≈5.

We are grateful for financial support from STFC (Grants No. ST/L000946/1, No. ST/N005406/1, and No. ST/M006913/1), the Royal Society (Grant No. RG110331), and the University of the West of Scotland, Strathclyde and Glasgow. I. W. M. is supported by a Royal Society Research Fellowship. Z. T. is supported by the European Commission under the FP7 Marie Curie ITN project "GraWIToN." We are grateful to the International Max Planck Partnership for Measurement and Observation at the Quantum Limit for support, and we thank our colleagues in the LSC and VIRGO collaborations and within SUPA for their interest in this work. We are grateful for technical support from Liz Porteous, Gerry O'Hare, Andy Bunyan, Colin Craig, Jacob Bell, and Margarette Kupsch and to M. Ende for inspiration. This Letter has LIGO document number LIGO-P1800148.

*Ross.Birney@strath.ac.uk
†Jessica.Steinlechner@ligo.org

[1] F. Riehle, Nat. Photonics **11**, 25 (2017).
[2] A. Bauch, Meas. Sci. Technol. **14**, 1159 (2003).
[3] A. Derevianko and M. Pospelov, Nat. Phys. **10**, 933 (2014).
[4] B. P. Abbott *et al.*, Phys. Rev. Lett. **116**, 061102 (2016).
[5] B. P. Abbott *et al.*, Phys. Rev. Lett. **116**, 241103 (2016).
[6] B. P. Abbott *et al.*, Phys. Rev. Lett. **118**, 221101 (2017).
[7] B. P. Abbott *et al.*, Phys. Rev. Lett. **119**, 141101 (2017).
[8] D. G. Matei *et al.* Phys. Rev. Lett. **118**, 263202 (2017).
[9] B. P. Abbott *et al.*, Phys. Rev. Lett. **116**, 131103 (2016).
[10] R. Flaminio, J. Franc, C. Michel, N. Morgado, L. Pinard, and B. Sassolas, Classical Quantum Gravity **27**, 084030 (2010).
[11] G. M. Harry, M. R. Abernathy, A. E. Becerra-Toledo, H. Armandula *et al.*, Classical Quantum Gravity **24**, 405 (2007).
[12] P. G. Murray, I. W. Martin, K. Craig, J. Hough, R. Robie, S. Rowan, M. R. Abernathy, T. Pershing, and S. Penn, Phys. Rev. D **92**, 062001 (2015).
[13] X. Liu, B. E. White, Jr., R. O. Pohl, E. Iwanizcko, K. M. Jones, A. H. Mahan, B. N. Nelson, R. S. Crandall, and S. Veprek, Phys. Rev. Lett. **78**, 4418 (1997).
[14] J. Steinlechner, A. Khalaidovski, and R. Schnabel, Classical Quantum Gravity **31**, 105005 (2014).
[15] J. Steinlechner, I. W. Martin, R. Bassiri, A. Bell, M. M. Fejer, J. Hough, A. Markosyan, R. K. Route, S. Rowan, and Z. Tornasi, Phys. Rev. D **93**, 062005 (2016).
[16] J. Steinlechner, I. W. Martin, A. S. Bell, J. Hough, M. Fletcher, P. G. Murray, R. Robie, S. Rowan, and R. Schnabel, Phys. Rev. Lett. **120**, 263602 (2018).
[17] W. B. Jackson and N. M. Amer, Phys. Rev. B **25**, 5559 (1982).
[18] https://www.polygonphysics.com, Grenoble, France.
[19] R. Geller, *Electron Cyclotron Resonance Ion Sources and ECR Plasmas* (Institute of Physics Publishing, Bristol, 1996).
[20] J. M. E. Harper, in *Thin Film Processes*, edited by J. L. Vossen and W. Kern (Academic Press, New York, 1978), pp. 175–206.
[21] I. G. Brown, P. Spaedtke, R. Hollinger, P. Spaedtke, R. Hollinger, N. V. Gavrilov, M. Farley, P. Rose, G. Ryding, K.-N. Leung, N. Sakudo, C. Lyneis, D. Leitner, B. Sharkov, E. Oks, J. Ishikawa, J. Kwan, and Y. Takeiri, *The Physics and Technology of Ion Sources*, edited by I. G. Brown (Wiley-VCH Verlag GmbH & Co KGaA, Weinheim, 2004).
[22] B. Lewis and D. S. Campbell, J. Vac. Sci. Technol. **4**, 209 (1967).
[23] M. J. Stowell, Philos. Mag. **21**, 125 (1970).
[24] V. A. Volodin and D. I. Koshelev, J. Raman Spectrosc. **44**, 1760 (2013).
[25] Corning HPFS 7979 IR-grade fused silica, https://tinyurl.com/ybu4htbt.
[26] Knight optical UV-grade fused silica JGS1, https://www.knightoptical.com.
[27] A. L. Alexandrovski, M. M. Fejer, A. Markosyan, and R. Route, Proc. SPIE Int. Soc. Opt. Eng. **7193**, 71930D (2009).
[28] O. S. Heavens, *The Optical Properties of Thin Solid Films* (Dover Publications Inc., New York, 1992).
[29] P. J. Zanzucchi, C. R. Wronski, and D. E. Carlson, J. Appl. Phys. **48**, 5227 (1977).
[30] G. R. Eaton, S. S. Eaton, D. P. Barr, and R. T. Weber, *Quantitative EPR* (Springer-Verlag, Wien, 2010).
[31] D. R. Queen, X. Liu, J. Karel, T. H. Metcalf, and F. Hellman, Phys. Rev. Lett. **110**, 135901 (2013).
[32] D. R. Queen, X. Liu, J. Karel, H. C. Jacks, T. H. Metcalf, and F. Hellman, J. Non-Cryst. Solids **426**, 19 (2015).
[33] W. Theiss, SCOUT Software, http://www.wtheiss.com/.
[34] O. Stenzel, *The Physics of Thin Film Optical Spectra*, Springer Series in Surface Sciences, Vol. 44, 2nd ed. (Springer, Berlin, 2016), pp. 47–83.
[35] S. K. O'Leary, S. R. Johnson, and P. K. Lim, J. Appl. Phys. **82**, 3334 (1997).
[36] S. J. Youn, T. H. Rho, B. I. Min, and K. S. Kim, Phys. Status Solidi B **244**, 1354 (2007).
[37] J. Singh, Phys. Rev. B **23**, 4156 (1981).

[38] P. K. Giri, S. Tripurasundari, G. Raghavan, B. K. Panigrahi, P. Magudapathy, K. G. M. Nair, and A. K. Tyagi, J. Appl. Phys. **90**, 659 (2001).
[39] G. Vajente, R. Birney, A. Ananyeva *et al.*, Classical Quantum Gravity **35**, 075001 (2018).
[40] S. Gras and M. Evans, arXiv:1802.05372.
[41] L. Pinard, C. Michel, B. Sassolas, L. Balzarini, J. Degallaix, V. Dolique, R. Flaminio, D. Forest, M. Granata, B. Lagrange, N. Straniero, J. Teillon, and G. Cagnoli, Appl. Opt. **56**, C11 (2017).
[42] A. Brooks (private communication).
[43] A. F. Brooks, B. Abbott, M. A. Arain *et al.*, Appl. Opt. **55**, 8256 (2016).
[44] J. Steinlechner, I. W. Martin, J. Hough, C. Kruger, S. Rowan, and R. Schnabel, Phys. Rev. D **91**, 042001 (2015).
[45] W. Yam, S. Gras, and M. Evans, Phys. Rev. D **91**, 042002 (2015).
[46] M. E. Zucker, in Proceedings of LIGO Dawn Workshop, https://dcc.ligo.org/LIGO-G1601435/public.